Competition between multiphoton fragmentation channels in H_2 and HD induced by intermediate states

W. T. Hill III, B. P. Turner,* S. Yang, J. Zhu, and D. L. Hatten
Institute for Physical Science and Technology, University of Maryland, College Park, Maryland 20742
(Received 14 September 1990)

The proton and deuteron spectra following resonant multiphoton ionization of H_2 and HD at 193 nm through the E,F state have been studied at power densities of 10^{10} W/cm^2. Our results show that the intermediate state induces competition between 3(2+1)-photon ionization, dissociation, and dissociative ionization channels. We find that the competition depends on the specific vibrational and rotational levels excited in the intermediate state. At the same time, the mere presence of this bound intermediate state renders these three-photon fragmentation channels so efficient that higher-order fragmentation processes, such as Coulomb explosions requiring many more photons, are not observed.

I. INTRODUCTION

Recently, there have been several reports of intense-field ($\geq 10^{14}$ W/cm^2) multiphoton-ionization experiments designed to see double ionization of H_2 and its isotopes at close range (the equilibrium internuclear distance).[1-3] Such double ionization occurs about 50 eV above the ground state and generally requires the absorption of many (typically eight or more) photons. The two bare protons that would be generated would be less than 1 Å apart and would repel each other, leading to a rapid dissociation that has come to be known as a Coulomb explosion. The bulk of the results reported show no evidence for such events in H_2.[4] Codling, Frasinski, and Matherly[1] suggested that the reason it may be difficult to observe Coulomb explosions in hydrogen may be due to dissociation or dissociative ionization that can occur with many fewer photons during the early, low-intensity portion of the laser pulse. This hypothesis is substantiated by contemporary theoretical[5] and low-intensity experimental[6] studies that have shown that competition between ionization and dissociation channels is fundamental to the decay dynamics in highly excited diatomic systems. In some instances, dissociation will completely dominate ionization.[7]

This competition can be enhanced in multiphoton experiments because of intermediate states that can alter the partitioning between ionization and dissociation. For example, the two-photon resonant three-photon ionization experiments at low intensities ($\leq 10^9$ W/cm^2) by Buck, Parker, and Chandler[8] on H_2 showed that the ratio between dissociative ionization products,

$$nh\nu + H_2 \rightarrow H + H^+ + e^- ,$$

and ionization products,

$$nh\nu + H_2 \rightarrow H_2^+ + e^- ,$$

depends upon the specific intermediate state excited. These authors did not measure the kinetic-energy spectrum of the protons, however. We have measured the kinetic-energy spectra of protons and deuterons subsequent to excitation of H_2 and HD by an ArF* excimer laser (pulse length ≈ 15 ns, power density $\approx 10^{10}$ W/cm^2) tuned to specific intermediate vibrational and rotational states of the E,F potential of H_2 and HD. The goal of our study was to determine whether intermediate states can cause low-order fragmentation processes that lead to low-energy protons, to inhibit higher-order processes that lead to very energetic protons.

II. APPARATUS

The apparatus employed in this study is described in detail in Ref. 9 and only key elements will be pointed out here. Fragmentation of H_2 and HD (97% purity, with 1.5% each of H_2 and D_2, purchased from Cambridge Isotope Laboratory) was induced by an ArF^* (193-mn) excimer laser that was either line-narrowed ($\Delta\nu \approx 0.75$ cm^{-1}) and tuned to the two-photon $Q(0)$ line of the $E,F\ ^1\Sigma_g^+(v=6,J=0) \leftarrow X\ ^1\Sigma_g^+(v=0,J=0)$ transition in H_2 at 51 780 cm^{-1} or operated broadband ($\Delta\nu \approx 150$ cm^{-1}, $\nu_0 \approx 51\,750$ cm^{-1}), thus exciting the $Q(0)$ and $Q(1)$ lines. Power densities of the order of 10^{10} W/cm^2 were achieved with this laser when focused with a 500-mm lens. Our laser beam was only slightly polarized with a 60/40 ratio between the two orthogonal components.

The mass and kinetic energies of the ionic fragments were measured with a time-of-flight (TOF) ion detector and a 1-gigasample/s digitizing oscilloscope. The ion detector was composed of extraction and acceleration regions, a 55-cm field-free drift region and a pair of microchannel plates (MCP) to convert the ion pulses into electron pulses. The potential difference in the extraction region was between 0 and 30 V while in the acceleration region it was between 50 and 200 V. Kinetic energies were estimated from the flight times via computer simulation of the trajectories, as discussed in Ref. 9. The absolute time and zero kinetic energy were calibrated by the flight times of H_2^+ and HD^+ ions. The resolution (which we

assumed was due solely to the 15-ns pulse length of the laser) and the collection efficiency of the instrument varied with the kinetic energy of the ion and the extraction and acceleration potentials. Typically, the resolution ranged from 0.1–0.2 eV or less for kinetic energies less than 1 eV to about 0.3–0.5 eV for kinetic energies of ≈ 4 eV. For our operating conditions, the solid angle subtended by our TOF detector at the laser focus was small ($\approx 1.5\times 10^{-3}$ sr). Consequently, the collection efficiency fell rapidly from nearly 100% at 0 eV kinetic energy to about 5% at 1 eV and then more slowly to about 1% at 10 eV.

Dispersed fluorescence measurements with a resolution of ≈ 0.1 nm also were made with a $\frac{3}{4}$-m Spex monochromator. The fluorescence signal was monitored with a Hamamatsu R928 photomultiplier and then digitized with a charge sensitive analog-to-digital converter or the digital oscilloscope (to make time-resolved measurements).

III. EXPERIMENT

The potential-energy curves germane to our discussion are sketched in Fig. 1. These include the $X\,^1\Sigma_g^+[(1s\sigma_g)^2]$ ground and the $E,F\,^1\Sigma_g^+[1s\sigma_g 2s\sigma_g+(2p\sigma_u)^2]$ excited potentials of H_2 given by Sharp,[10] the lowest doubly excited autoionizing Rydberg potential, $^1\Sigma_u^+(2p\sigma_u 2s\sigma_g)$, converging to the $^2\Sigma_u^+(2p\sigma_u)$ state of H_2^+ calculated by Guberman[11] and the two lowest potential curves of H_2^+ also taken from Sharp. The dot-filled region between the $^1\Sigma_u^+$ doubly excited neutral state and the $^2\Sigma_u^+$ excited ion state correspond to a range containing Rydberg series composed of doubly excited neutral states converging to the $^2\Sigma_u^+$ excited ion state. The electronic curves of HD are identical to those shown in Fig. 1 albeit the gerade and ungerade labels are not strict in this case.

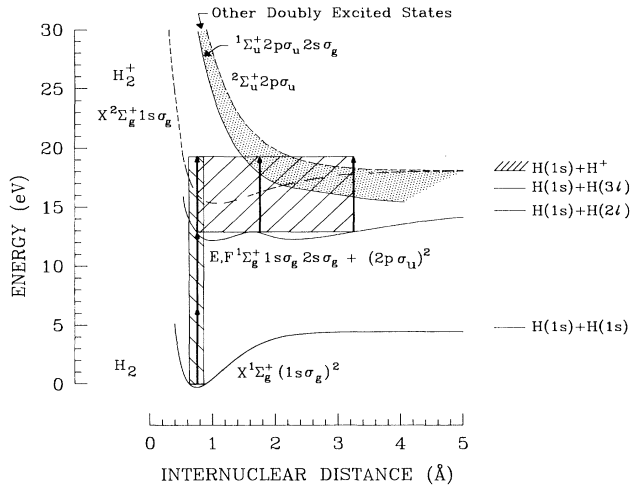

FIG. 1. Selected potential curves of H_2 and H_2^+. The solid and dashed curves correspond to the neutral and ionized molecules respectively and are drawn from the data of Sharp (Ref. 10). Doubly excited states of H_2, calculated by Guberman (Ref. 11) that converge to the $^2\Sigma_u^+(2p\sigma_u)$ state of H_2^+ are located in the dotted region between the $^1\Sigma_g^+(2p\sigma_u 2s\sigma_g)$ and $^2\Sigma_u^+(2p\sigma_u)$ curves. Several neutral dissociation thresholds are indicated to the right of the molecular curves. The arrows represent a 6.4-eV (193-nm) photon. The forward-hatched horizontal rectangular area indicates the approximate range of internuclear distances over which excitations from the E,F state can occur; the backward-hatched vertical rectangular area indicates the region of maximum amplitude of the ground-state wave function.

Coulomb explosion events correspond to vertical transitions in which the internuclear separation stays within the range specified by the backward hatched rectangular area in Fig. 1. For the wavelength of our laser, 193 nm ($h\nu=6.4$ eV), the double-ionization limit requires at least eight photons and will be identified by very energetic protons and deuterons. Table I gives the expected kinetic energies for H^+ and D^+ resulting from Coulomb explosion events in H_2 and HD. The values in Table I were calculated at the equilibrium distance of the ground state, approximately 0.74 Å.

When we excite an eigenstate of the E,F state near the top of the barrier, we must take into account the fact that the vibrational wave function of the levels may have appreciable amplitude in both wells. As this is the case for $v_{E,F}=6$ and 7,[12–14] the allowed internuclear separation of the molecules in the E,F state extends out to 3 Å as opposed to only 1 Å as it would be for molecules in the ground state. Further photoexcitation of molecules that are in this intermediate state takes place over the internuclear distances indicated by the forward-hatched horizontal rectangular area in Fig. 1. Three regions of the structure can be reached that lead to 3(2+1)-photon fragmentation events. We define these regions as follows: region I, the bound portion of the $X\,^2\Sigma_g^+$ state of H_2^+ (HD^+) and its dissociation continuum; region II, the dissociating doubly excited autoionizing Rydberg states of H_2 (HD), the dotted region in Fig. 1, based on the $^2\Sigma_u^+$ core of H_2^+ and HD^+; region III, the dissociation continuum of H_2^+ above the $^2\Sigma_u^+$ state. These regions are reached sequentially as the intermediate separation of the molecule increases. Thus, three-photon excitation of H_2 (HD) to states 19.2 eV above the ground state will induce mutual competition between ionization (which we will refer to as channel I), dissociation (channel II), and dissociative ionization (channel III), and could impede higher-order frag-

TABLE I. Coulomb explosion energies and ion times of flight.

	Ion	Energies (eV)[a]	TOF (μs)[a,b]
H_2	H^+	9.73	2.82
HD	H^+	12.97	2.79
	D^+	6.49	4.04

[a]These values were calculated at the equilibrium position of the ground state, ≈ 0.74 Å.

[b]These values were calculated assuming the experimental conditions of Figs. 1 and 2.

mentation processes as well. Channel I includes both direct ionization (which opens first at close range, region I) and autoionization (region II). Channel II involves those molecules which survive autoionization in region II while channel III is due to the repulsive portion of the ground potential of the ion (region I) as well as the continuum above the $2p\sigma_u$ potential of the ion (region III).

Each of these channels leads to a characteristic proton and/or deuteron energy spectrum. For channel I, in the case of H_2, we have the three-photon fragmentation process

$$3h\nu_{193}+H_2\rightarrow H_2^+[v,J]+e^- . \quad (1)$$

This is followed by a probe step

$$h\nu_{193}+H_2^+[v,J]\rightarrow H(1s)+H^+ . \quad (2)$$

The excess photon energy in (2) is shared equally between $H(1s)$ and H^+; the kinetic energy of H^+, in this case, will range from 1.88 to 3.20 eV, depending on v of the molecular ion generated in (1). For channel II, we have

$$3h\nu_{193}+H_2\rightarrow H(1s)+H(nl), \quad (3)$$

followed by the probe step

$$h\nu_{193}+H(nl)\rightarrow H^+ +e^- . \quad (4)$$

The possible kinetic energies that H^+ can acquire in (4) range from 0.56 to 2.25 eV, depending on the value of n (≥ 2) for $H[nl]$ generated in (3). Finally, for channel III we have

$$3h\nu_{193}+H_2\rightarrow H(1s)+H^+ +e^- . \quad (5)$$

The excess photon energy is shared among the three fragments with H^+ and $H(1s)$ having nearly equal energy. This time, the possible range of kinetic energy for H^+ will be 0–0.56 eV. A corresponding analysis for the HD case, involving twice as many expressions, can be done to determine the allowed kinetic energy ranges for H^+ and D^+.

There is a fourth channel that should be open via three-photon excitation as well. Namely, dissociation into the ion pair

$$3h\nu_{193}+H_2\rightarrow H^+ +H^- . \quad (6)$$

Sharp[10] gives a value of 17.3 eV for the threshold for generation of the ion pair. We would expect to see a rather narrow peak at 0.95 eV representing these protons if this channel were active.

IV. RESULTS AND INTERPRETATION

The upper trace of Fig. 2 shows a typical TOF spectrum of the charged fragments following photoexcitation of H_2 in which one observes a single H_2^+ peak and several H^+ peaks. A similar spectrum taken under the same conditions is shown in the lower trace of Fig. 2 for HD. For HD, one observes several peaks each for H^+ and D^+ and a very weak HD^+ peak; weak HD^+ peaks were typical in all of our HD TOF spectra. The maximum ion signal in HD was about half the maximum signal in H_2.

The atomic fragments in Fig. 2 have a fast and a slow component. The peaks marked *F* (fast) and *S* (slow) are due to ions that are initially directed toward the detector and are the ones we analyzed. The third and fourth peaks (marked with a *B* for backwards) in the upper trace correspond to fast and slow protons initially directed away from the detector that must be turned around by the field to be detected.[15] For HD, only one of the backward peaks is large enough to be observed. The dashed line in Fig. 2 shows that the slow D^+ peak does not occur at 0 eV. We thus conclude this slow peak is not due to H_2^+ impurity since H_2^+ peaks at 0 eV.

We have plotted the relative atomic ion yields (taken from Fig. 2) versus energy in Fig. 3, with 0 representing 0 eV initial kinetic energy. The allowed ranges of kinetic

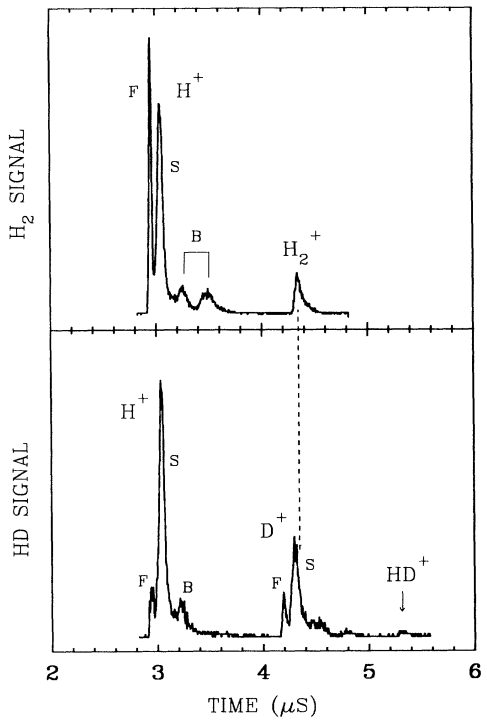

FIG. 2. Typical TOF ion spectra following photofragmentation of H_2 (upper panel) and HD (lower panel) taken with the laser broadband. The peaks marked with *F*, *S*, and *B* indicate fast, slow, and backward components respectively (see text). Experimental parameters (see Ref. 9 for a description) are $V_{12}=15$, V, $V_{23}=200$ and -2000 V on the front MCP; 4×10^{-6} Torr of H_2 or HD; voltage digitized every 4 ns for H_2 and every 5.5 ns for HD. Under these conditions, the HD^+ peak in the lower panel occurs at 5.30 μs. Each spectrum is a composite of 60 laser shots. The spectra displayed are typical of both broadband and narrow-band excitation. When the laser was narrow band and tuned a few wave numbers off resonance, the ion signal was about the same strength as shown here; when the laser was tuned on resonance the signal was about five times larger.

energies for channels I–III have been indicated in the figure as well. Note that Fig. 3 has been truncated before the energies at which Coulomb explosion events occur because we do not observe any ions in Fig. 2 corresponding to the times of flight given in Table I for these events. The fast ion peaks are greatly enhanced relative to the slow peaks because of the precipitous drop in the collection efficienty with increasing kinetic energy between 0 and 1 eV. To determine the relative yields we had to correct for this drop. If we assume that the angular distribution of the fragments is isotropic, it is straightforward to calculate the collection efficiency as a function of energy from a point source. With additional effort, it is possible to account for ions created along a short line segment collinear with the laser beam as well. Under our experimental conditions, however, the energy-dependent collection efficiency for the line segment case is not much different from that for the point source case; the ion yields in Fig. 3 are based on a point source calculation. Our assumption that the distribution is isotropic is valid in our case because our laser was only slightly polarized and the TOF spectra with the laser polarized parallel and perpendicular to the TOF axis were nearly the same.

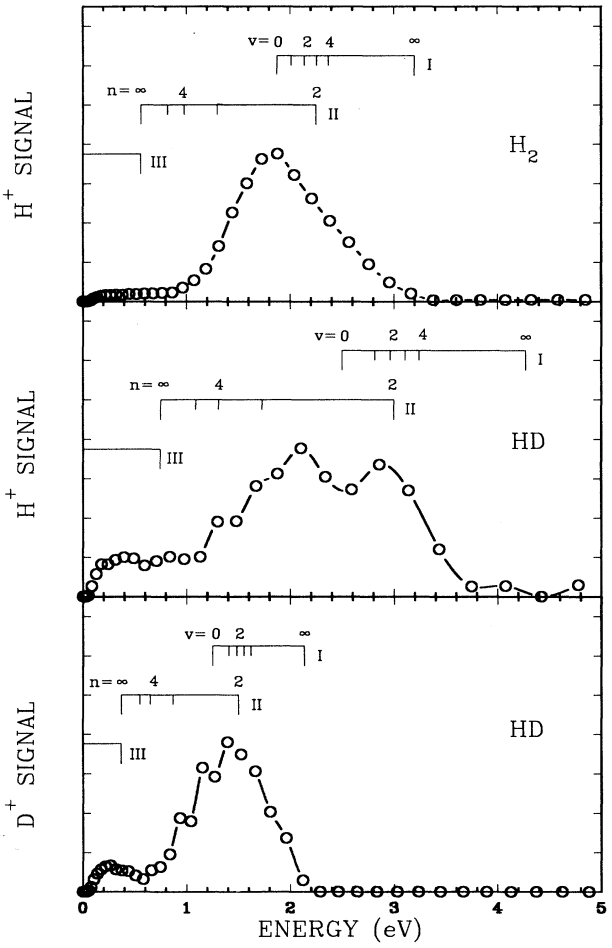

FIG. 3. Relative ion yields vs initial kinetic energies for H^+ and D^+ taken from the TOF spectra of Fig. 2. Each trace has been corrected for collection efficiently as discussed in the text and plotted on a linear scale. The coordinate axis is the zero of the ordinate axis and represents the zero ion signal level. The ratio of peak yields from the top panel to the bottom panel is 13:2:1. The scale above each trace indicates the allowed ranges of kinetic energies for ionization (I), dissociation (II), and dissociative ionization (III).

Figure 3 shows that the three-photon fragmentation channels can account for the entire kinetic-energy spectra of the ions. We note first that the ions due to channel III (dissociative ionization) are clearly distinguishable from ions due to channels I and II. Hence the presence of very-low-energy atomic ions is evidence that dissociative ionization is an active channel at 193 nm in both H_2 and HD. Since the peak of the kinetic-energy spectrum falls at an energy where channels I and II overlap, we relied upon secondary observations to confirm that both of these channels were active. Unfortunately, we could not measure negative ions so we could not determine if ion pair dissociation contributed to the ions generated at 0.95 eV.

Our confidence that channel I (ionization) is active is based on the fact that (i) molecular ions are observed in our spectrum and (ii) the calculated photodissociation cross sections σ_{diss} are large enough that many of the molecular ions created via channel I will be dissociated by a fourth photon. For the low-lying vibrational levels of H_2^+, σ_{diss} is in the 10^{-18}-cm^2 range for $v=1-9$, when $v=0$, σ_{diss} is $\approx 5\times 10^{-20}$ cm^2 and when $v=5$, it is $\approx 10^{-19}$ cm^2.[16] Since our laser power density is of the order of 10^{10} W/cm^2, which corresponds to a photon density of about 1.5×10^{20} photon/cm^2 pulse, transitions from all of these levels will be saturated. The low-intensity photoelectron measurements by Anderson, Kubiak, and Zare[17] show that H_2^+ generated by 193-nm radiation results in a significant fraction of the ions in the low-v states. Thus it is very reasonable to conclude from our data that channel I is active.

Our observation of the first few members of the Balmer series of atomic hydrogen (Fig. 4) corroborates the fact that channel II (dissociation) is active. Since the quasiclassical photoionization cross section of $H(nl)$ at our photon frequency is $\approx 7.6\times 10^{-17}/n^5$ cm^2,[18] the photoionization transition for atoms in states with $n=2-6$ (created via dissociation) will be saturated. The Balmer series was observed with as little as 10 mTorr of H_2 in the vacuum chamber. At 10 mTorr, the mean free path of neutral room temperature hydrogen is about 2 cm so there will be less than one collision during the laser pulse (≈ 15 ns). All the fluorescence components began with the leading edge of the laser pulse and terminated just prior to the end of the pulse. However, the spontaneous lifetimes of these excited levels vary by more than an order of magnitude from $n=3$ to 6; they range from about 10 ns for $n=3$ to about 193 ns for $n=6$. These facts taken together are the basis of our evidence that the excited atomic hydrogen we observe fluorescing was generated by the laser and not by collisions. Although the atomic

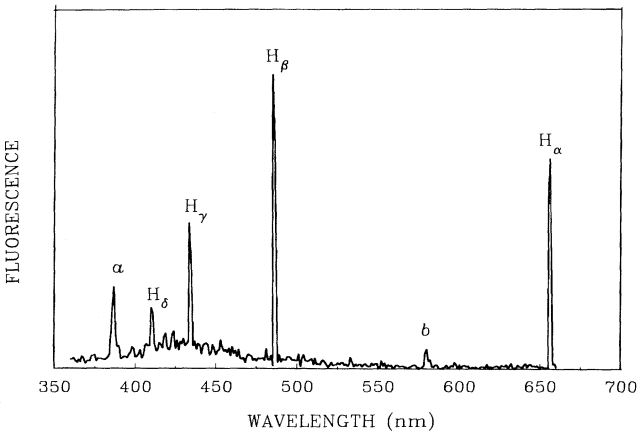

FIG. 4. First few members of the Balmer series of H observed in 100 mTorr of H_2. The peaks marked *a* and *b* are due to second- and third-order scattered laser light.

fluorescence is a clear signal of excited neutral atomic hydrogen, a combination of fluorescence cascading and premature termination of the signal (via photoionization), together with the fact that we could only detect atoms in $l=0$, 1, and 2 angular momentum states (we were blind to the higher l states for $n>3$), prevented us from using the fluorescence signal to determine the nascent population in the various excited levels produced by dissociation (channel II).

There are two observations we can make from Figs. 2 and 3. The first is that the distribution of strength between the three channels is different for HD and H_2. The second is that the three-photon fragmentation channels are very efficient at our power densities. If Coulomb explosion events do occur, they must be at least three or four orders of magnitude less frequent. Both of these observations can be linked to the structure of the intermediate E,F state.

In general, the vibrational wavefunctions of the E,F state exist in both wells simultaneously. However, depending on v and J of the level, the wave will usually be more localized in one well or the other. When $v_{E,F}=0$, 3, and 6, the wave function is nominally assigned to the E well, whereas for values of 1, 2, 4, 5, and 7 it is assigned to the F well.[14] Near $v_{E,F}=6$ and 7, the system is strongly mixed; for low J, the E and F wells can be associated with $v_{E,F}=6$ and 7, respectively. Above a certain J, however, the character switches. The *ab initio* calculations of Ref. 13 show that this tranistion occurs about 103 895.6 cm^{-1} above the ground state of H_2, which corresponds to an energy between $J=2$ and 3. Plots of theoretical vibrational wave functions for various J levels for $v_{E,F}=6$ and 7 by Senn *et al.*[13] corroborate this by showing that the probability of finding the system in the E well is high for $v_{E,F}=6$, $J<2$ and for $v_{E,F}=7$, $J>3$. When $J=2$ or 3 for either $v_{E,F}=6$ or 7, the probability of finding the system in either well is about 50%. When we excite the $J=0$ and 1 levels of $v_{E,F}=6$ in H_2, we must consider transitions corresponding to a wave function that is localized predominantly in the E well.

When the vibrational wave function is localized in the E well, the dominant transitions (which correspond to channel I in a single-particle picture would be

$$h\nu_{193}+H_2(1s\sigma_g 2s\sigma_g)\rightarrow H_2^+(1s\sigma_s)+e^-(\epsilon l\lambda_\mu)\ . \tag{7}$$

The H_2^+ will be bound permanently or will dissociate spontaneously depending on how much energy the electron carries off. At the same time, we would expect the transition probabilities to excite H_2 to final states based upon $2p\sigma_u$ H_2^+ core states, such as the doubly excited states of region II and the dissociating states of region III to be smaller. This will be due to the fact that the nuclear wave functions for the states in regions II and III (at 19.2 eV) have very little overlap with a wave function localized in the E well. Furthermore, excitation to states in regions II and III from a $1s\sigma_g 2s\sigma_g$ state (the E portion) to $2p\sigma_u nl\lambda_g$ states will require both electrons to be excited by a single photon.

For HD, however, the same *ab initio* calculations of Ref. 14 show that the transition in character from the E well to the F well occurs between $J=3$ and 4, 103 581.5 cm^{-1} above the ground states. The $Q(0)$ and $Q(1)$ transition we excite will put HD in the $v_{E,F}=7$, $J=0$ and 1 states, which will have more F character than E character. A single-particle picture would suggest that the strongest transitions from an F well level would be

$$h\nu_{193}+HD(2p\sigma_u^2)\rightarrow \begin{cases} HD^*(2p\sigma_u nl\lambda_g) \\ HD^+(2p\sigma_u)+e^-(\epsilon l\lambda_g)\ . \end{cases} \tag{8}$$

One can argue again that transitions to final states based on the $1s\sigma_g HD^+$ core (region I) could be weaker because they will require both electrons to be excited. Fragmentation described by (8) will contribute to all three channels.

Since we do not have pure single-particle states, all three channels will be active in both H_2 and HD, as we observe. The $^2\Sigma_u^+(2p\sigma_u)$ dissociation continuum can be reached more efficiently in HD than in H_2, due to the vibrational wave function being more localized in the F well for HD, which would explain why we observe more ions associated with channel III relative to channels I and II.[19] More quantitatively, we see that the ratio of the integrated charge Γ is about 0.02 ± 0.01 for H_2 and 0.12 ± 0.06 for HD, where we define Γ as

$$\Gamma\equiv\frac{C_{\rm III}}{C_{\rm I}+C_{\rm II}}\ , \tag{9}$$

where $C_{\rm III}$ represents the integrated charge for channel III, while $C_{\rm I}$ and $C_{\rm II}$ represent the integrated charge for channels I and II, respectively. Figures 2 and 3 suggest that the contribution of channel II relative to channel I is larger in HD than in H_2 as well. Note that H^+ and D^+ signals extend to higher n values (channel II) in Fig. 3. Compare, as well, the relative size of the H_2^+ and the HD^+ peaks with the slow H^+ and D^+ peaks in Fig. 2.

It is instructive to compare our results with recent related experiments. At the intense-field extreme (and at

wavelengths different from ours), it is interesting to note that the maximum kinetic energies observed for the protons and deuterons (from D_2) were only 5 or 6 eV, too low to be due to Coulomb expolosion events.[1-3] Bucksbaum *et al.*[3] suggest a stepwise mechanism in which H_2 is first ionized and then H_2^+ undergoes "above-threshold dissociation"[20] (ATD) leading to $H+H^+$, with H^+ having energies less than those expected for Coulomb explosion events. At the low-intensity extreme, Buck, Parker, and Chandler[8] measured the ratio of H^+/H_2^+ (without distinguishing the H^+ kinetic energies) for two-photon resonant three-photon fragmentation of H_2 through the $v_{E,F}=6$ and 7 levels and found that it depended upon J as well. In contrast to their conclusion, however, we do find that dissociation of H_2^+ is an important process and contributes to the H^+ signal. The discrepancy between their result and ours may be associated with the fact that their measurements were done at power densities much lower than ours. They do not give an estimate of their power density at the beam focus. We estimate from the information they provide that their power density is 10 to 100 times less than ours. Finally, single-photon experiments with 64.3-nm radiation, corresponding to three 193-nm photons, show that the dominant transition involves excited states that have wave functions with appreciable amplitude in region I.[21] In the one-photon experiments, the lower level wave function is restricted to the backward hatched rectangular box of Fig. 1, so there will be very little overlap with states in regions II and III.

V. CONCLUSION

At our moderate intensities, the E,F intermediate state evidently reduces the probability of vertical transitions by delocalizing the wave packet describing the nuclear motion such that new channels of fragmentation open at large internuclear separations. In general, these channels open at lower excitation energies compared with the energies required for double ionization at short internuclear distances (leading to Coulomb explosions). Consequently, at large internuclear distances only a few photons are required to break up the molecule. In addition to the ATD suspected at high intensities, we expect that dissociation and dissociative ionization of the kind discussed in this paper to compete with double ionization as well. This is reasonable because (i) the wave packet describing the nuclear motion, upon excitation of the molecule to the intermediate state, develops faster than the typical pulse length (≥ 0.5 ps) lasers employed in these experiments and (ii) the electronic and nuclear motion can be comparable in H_2 for high-lying Rydberg states (i.e., breakdown of the Born-Openheimer approximation). In addition to the gerade E,F state, the ungerade $B\ ^1\Sigma_u^+(1s\sigma_g 2p\sigma_u)$ state can act as an intermediate state below the ionization limit. At longer wavelengths, three photons can be in near resonance with the B state, which can sustain a wave function over a wide range of internuclear distances as well. Furthermore, since the intensity of a laser pulse varies spatially, one is virtually assured to be near resonance with some intermediate state via Stark shifting.[22] Finally, there is an infinite set of doubly excited Rydberg states converging to the various dissociation limits below the double-ionization limit that can cause dissociation or dissociative ionization prior to double ionization. It is, thus, very tempting to suggest that bound and dissociating intermediate states help to impede the observation of Coulomb explosion events in H_2 and its isotopes even in intense-field experiments. We are planning to perform similar experiments with intense ($\geq 10^{13}$ W/cm^2) picosecond radiation at 193 nm to explore this point further.

ACKNOWLEDGMENTS

We acknowledge helpful discussions with Dr. J. Cooper, Dr. M. L. Ginter, Dr. A. Giusti-Suzor, and Dr. F. Mies, and technical support from Mr. A. Pinkas. This work was sponsored by the National Science Foundation through Grant Nos. PHY-84 06192 and PHY-84 51284.

*Current address: Fusion Systems Corporation, 7600 Standish Place, Rockville, MD 20885.

[1]K. Codling, L. J. Frasinski, and P. A. Hatherly, J. Phys. B **21**, L433 (1988).

[2]T. S. Luk and C. K. Rhodes, Phys. Rev. A **38**, 6180 (1988).

[3]P. H. Bucksbaum, A. Zavriyev, H. G. Muller, and D. W. Schumacher, Phys. Rev. Lett. **64**, 1883 (1990).

[4]The sole exception is an experiment performed at power densities of about 10^{11} W/cm^2 with a 308-nm excimer laser (pulse length $\approx$28 ns) by M. H. Nayfeh, J. Mazumder, D. C. Humm, T. Sherlock, and K. Ng, in *Atomic and Molecular Processes with Short Intense Laser Pulses,* edited by A. B. Bandrauk (Plenum, New York, 1988), p. 177.

[5]See, for example, Ch. Jungen, Phys. Rev. Lett. **53**, 2394 (1984); W. A. Chupka, J. Chem. Phys. **87**, 1488 (1987); A. Giusti-Suzor and Ch. Jungen, *ibid.* **80**, 986 (1984).

[6]See, for example, C. Cornaggia, A. Giusti-Suzor and Ch. Jungen, J. Chem. Phys. **87**, 3934 (1987); M. A. O'Halloran, S. T. Pratt, P. M. Dehmer, and J. L. Dehmer, *ibid.* **87**, 3288 (1987); M. G. While, G. E. Leroi, M.-H. Ho, and E. D. Poliakoff, *ibid.* **87**, 6553 (1987).

[7]W. T. Hill III, B. P. Turner, H. Lefebvre-Brion, S. Yang, and J. Zhu, J. Chem. Phys. **92**, 4272 (1990).

[8]J. D. Buck, D. H. Parker, and D. W. Chandler, J. Phys. Chem. **92**, 37 (1988).

[9]B. P. Turner, W. T. Hill III, S. Yang, J. Zhu, A. Pinkas, and L. Bao, Rev. Sci. Instrum. **61**, 1182 (1990).

[10]T. E. Sharp, At. Data **2**, 119 (1971).

[11]S. L. Guberman, J. Chem. Phys. **78**, 1404 (1983).

[12]W. M. Huo and R. L. Jaffe, Chem. Phys. Lett. **101**, 463 (1983).

[13]P. Senn, P. Quadrelli, K. Dressler, and G. Herzberg, J. Chem. Phys. **83**, 962 (1985).

[14]P. Senn and K. Dressler, J. Chem. Phys. **87**, 1205 (1987).

[15]The peaks due to the backward-going ions are always smaller in our spectra. This is due in part to a smaller acceptance angle for the backward-going ions relative to the forward-going

ions.

[16]G. H. Dunn, Phys. Rev. **172**, 1 (1968). For complete tables see Joint Institute for Laboratory Astorphysics, Natural Bureau of Standards and University of Colorado Report No. 92, 1968 (unpublished).

[17]L. Anderson, G. D. Kubiak, and R. Zare, Chem. Phys. Lett. **105**, 22 (1984).

[18]R. D. Cowan, *Theory of Atomic Structure and Spectra* (University of California Press, Berkeley, 1981), p. 526.

[19]Since the electronic portion of HD and H_2 are nearly identical, we assume that the photoionization cross section of HD and the photodissociation cross section of HD^+ are about the same as the corresponding cross sections in the H_2.

[20]X. He, O. Atabek and A. Giusti-Suzor, Phys. Rev. A **38**, 5586 (1988); A. Giusti-Suzor, X. He, O. Atabek, and F. H. Mies, Phys. Rev. Lett. **64**, 515 (1990).

[21]R. Browning and J. Fryar, J. Phys. B **6**, 364 (1973); S. Strathdee and R. Browning, *ibid*, **12**, 1789 (1979).

[22]R. R. Freeman, P. H. Bucksbaum, H. Milchberg, S. Darack, D. Schumacher, and M. Geusic, Phys. Rev. Lett. **59**, 1092 (1987).